FUDMA Journal of Sciences (FJS)
ISSN online: 2616-1370
ISSN print: 2645 - 2944
Vol. 10 No. 13, July, 2026, pp 43 – 48
DOI: https://doi.org/10.33003/fjs-2026-1013-5503

Structural and Morphological Characterization of Graphene Oxide (GO), Reduced Graphene Oxide (rGO), and Nitrogen-Doped Graphene Oxide (N-GO) for Electrochemical Water Treatment

Alhassan Abidemi Bello, Abdul Dahiru Buba and *Abubakar Muhammad Ramalan

Department of Physics, University of Abuja, Abuja, Nigeria.

*Corresponding authors' email: abubakar.ramalan@uniabuja.edu.ng

Received: 11 Jul. 2026
Accepted: 17 Jul. 2026
Published: 3 Aug. 2026

ABSTRACT
Developing efficient electrode materials is essential for improving electrochemical water treatment technologies. In this study, we synthesized and compared three materials: graphene oxide (GO), reduced graphene oxide (rGO), and nitrogen-doped graphene oxide (N-GO). GO was produced using a modified Hummers method, followed by chemical reduction to obtain rGO and hydrothermal nitrogen doping to obtain N-GO. Scanning Electron Microscopy (SEM) showed clear morphological changes, evolving from the flat and exfoliated sheets of GO to the highly crumpled and porous three-dimensional structure of N-GO, which offers a larger surface area for contaminant adsorption. X-ray diffraction (XRD) confirmed an expanded interlayer spacing of about 0.86 nm in GO and the reappearance of the graphitic (002) peak near 25 degrees after reduction and nitrogen doping. Raman spectroscopy provided additional structural insights, showing a blue shift of the G band to around 1595 cm^{-1} and an ID/IG ratio of 1.11 in N-GO, indicating successful nitrogen incorporation and the formation of active defect sites. These combined structural improvements, especially the restored conductivity and increased defect density in N-GO demonstrate its strong electrochemical potential for removing pollutants from water. This work offers a solid structural foundation for designing optimized graphene-based electrodes for high-performance water purification systems.

Keywords: Graphene Oxide, N-doping, Hummers Method, Electrochemical Water Treatment, Structural Characterization

INTRODUCTION

Graphene-based materials continue to attract significant interest due to their exceptional structural tunability, large surface area, and favorable physicochemical properties that support a wide range of environmental and electrochemical applications (Dybowski et al., 2025). Among these materials, graphene oxide (GO), reduced graphene oxide (rGO), and nitrogen-doped graphene oxide (N-GO) represent three structurally distinct yet closely related carbon frameworks, each possessing unique functional groups, defect densities, and morphological features that influence their performance in electrochemical processes (Dreyer et al., 2010; Voiry et al., 2016). GO is characterized by abundant oxygenated functionalities, which impart hydrophilicity and high adsorption potential, whereas its reduced form, rGO, displays improved electrical conductivity and restored aromatic domains due to partial re-establishment of the sp^2 carbon network (Veleva, 2025; Stankovich et al., 2007). Nitrogen doping introduces additional defect sites and modifies the electronic structure, yielding materials with enhanced reactivity and stronger interactions with pollutants and electrolyte species (Geng et al., 2011; Qu et al., 2010).

These structural variations are particularly important for electrochemical water treatment, where electrode performance depends heavily on factors such as surface area, porosity, defect density, and the nature of functional groups. GO provides rich anchoring sites and strong affinity for contaminants but suffers from limited conductivity, while rGO offers improved charge transport properties critical for electron-driven oxidation and reduction reactions (Liu et al., 2018). N-GO combines the advantages of both materials: nitrogen functionalities generate catalytically active sites and modulate charge distribution, while the partially restored sp^2 network supports better conductivity and faster interfacial electron transfer (Li et al., 2022; Qu et al., 2010). These characteristics make N-GO a promising candidate for next-generation electrochemical water purification technologies.

Comprehensive characterization is therefore essential to understand how synthesis pathways modify the structural and morphological attributes of these materials. Raman spectroscopy provides insight into disorder, graphitization, and doping effects through analysis of the D, G, and 2D bands (Ferrari & Robertson, 2000). X-ray diffraction (XRD) reveals interlayer spacing changes associated with oxidation, reduction, and heteroatom doping (Pei & Cheng, 2012). Scanning electron microscopy (SEM) enables direct visualization of morphological transitions from the sheet-like laminar structure of GO to the wrinkled, porous, and crumpled architectures characteristic of rGO and N-GO (Zhou et al., 2014). Together, these techniques establish a structure–property relationship essential for predicting electrochemical performance.

In this study, we synthesize GO via a modified Hummers method and subsequently prepare rGO and N-GO through chemical reduction and hydrothermal nitrogen doping. We present a detailed structural and morphological comparison of these materials using Raman spectroscopy, XRD, and SEM. The findings provide fundamental insights into how oxidation, reduction, and nitrogen functionalization influence graphene-based frameworks and support their optimization for use as electrode materials in electrochemical water treatment systems.

MATERIALS AND METHODS

Experimental Method

Synthesis of Graphene Oxide (GO)

Graphene oxide was synthesized using a modified Hummers method. Graphite powder (1 g) was added to a beaker containing 23 mL of cold concentrated sulfuric acid maintained at approximately 10°C. Potassium permanganate (3 g) was introduced gradually while stirring to prevent excessive heat generation, and the temperature was kept below 20°C with an ice bath. After the oxidant was fully added, the mixture was stirred at 35°C for 2 hours to promote complete oxidation.

Deionized water (100 mL) was then added slowly, which caused a rise in temperature. The reaction was controlled and kept below 98°C using the ice bath. After 30 minutes, hydrogen peroxide solution (10 mL, 30 percent) was added until the mixture developed a yellow brown color, indicating the reduction of residual manganese species. The suspension was centrifuged at 4000 rpm for 10 minutes and the supernatant was discarded. The solid material was washed repeatedly with 1 M hydrochloric acid, followed by several washes with deionized water until the pH became neutral. The resulting GO paste was dried in an oven at 60°C.

Synthesis of Reduced Graphene Oxide (rGO)

Dry GO (100 mg) was dispersed in 100 mL of deionized water by ultrasonication for 30 minutes. Ascorbic acid (1 g) was added as a reducing agent, and the mixture was heated at 95°C under continuous stirring for 3 hours. The color gradually changed from brown to black, confirming the formation of rGO. The product was collected by centrifugation, washed thoroughly with deionized water, and dried at 60°C.

Synthesis of Nitrogen Doped Graphene Oxide (N-GO)

GO (100 mg) was dispersed in 100 mL of deionized water and sonicated for 30 minutes. Urea was added as the nitrogen source at a GO to urea mass ratio of 1 to 5. The mixture was transferred into a Teflon lined autoclave and heated at 180°C for 10 hours to facilitate hydrothermal doping. After cooling to room temperature, the product was collected by centrifugation and washed repeatedly with deionized water until the pH reached approximately 7. The material was dried at 60°C overnight.

Preparation of Thin Film Electrodes

Glass slides were cleaned with ethanol and deionized water, then dried at room temperature. Masking tape was used to define the coating area. Dispersions of GO, rGO, and N-GO (2 mg per mL) were prepared in deionized water, and a small volume of Nafion solution (approximately 4 µL per mL) was added to improve film adhesion. Each dispersion was drop cast onto the defined area of the glass slide using a volume of about 50 µL. The films were allowed to dry at room temperature and then heated at 80°C for 1 hour to improve film stability. Copper tape was applied to one end of each film to provide good electrical contact.

Characterization Techniques

Table 1: A summary of the Characterization Techniques Used

Technique	Instrument & Conditions	Purpose (with References)
Raman Spectroscopy	Raman microscope with 532 nm excitation laser and CCD detector.	To assess layer number (sharp 2D band), defect density (D band), and confirm monolayer graphene via G/2D intensity ratio (Zhou et al., 2024).
XRD	X-ray diffractometer using Cu Kα radiation (λ = 1.5406 Å), scan range 10°–80° (2θ).	To observe (002) graphitic peak (~26.5°) and assess crystallinity/few-layer stacking (Novoselov et al., 2004).
SEM	Field-emission SEM operated at 5–10 kV.	To examine surface morphology, grain boundaries, wrinkles, domain structure, and continuity (Li et al., 2009).

RESULTS AND DISCUSSION

This section presents the structural, morphological, and spectroscopic characteristics of the synthesized graphene-based materials. The analyses compare graphene oxide (GO), reduced graphene oxide (rGO), and nitrogen-doped graphene oxide (N-GO) to understand how oxidation, chemical reduction, and nitrogen incorporation influence their properties. The results highlight changes in functional groups, defect concentration, crystallinity, surface morphology, and overall material quality, providing insight into their suitability for electrochemical water treatment applications.

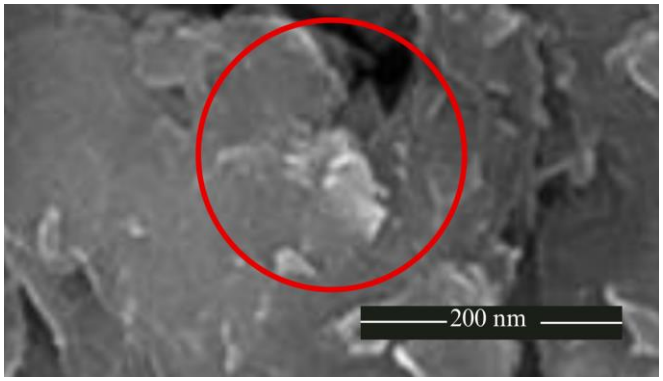

Figure 1: SEM image of Graphene Oxide Sample

The GO sample (figure 1) exhibits a highly layered and foliated structure. The presence of large, thin flakes indicates successful chemical exfoliation of the precursor graphite. The surface appears significantly wrinkled and crumpled (highlighted in the red circular region). These wrinkles are a hallmark of GO; they arise from the structural defects and the

introduction of oxygen-containing functional groups (such as epoxy and hydroxyl groups) during the aggressive oxidation process, which disrupt the sp^2 hybridization of the carbon plane. The individual surface features and folds are observed to be on the nanometer scale, while the lateral dimensions of the primary flakes extend beyond the current field of view, confirming the production of high-aspect-ratio nanosheets.

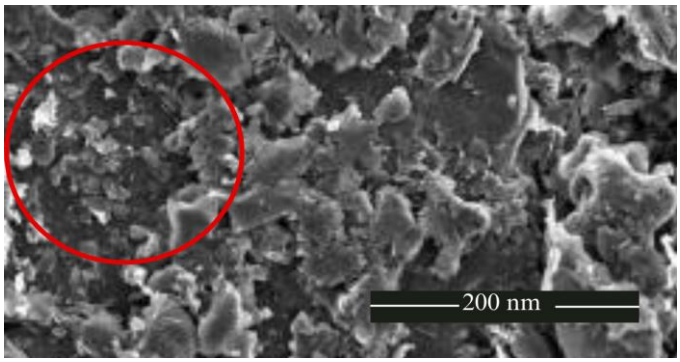

Figure 2: SEM image of Reduced Graphene Oxide Sample

In figure 2, the rGO sheets appear as thin, randomly aggregated flakes with a multi-layered stacking arrangement. This denser stacking, compared to GO, is attributed to the removal of oxygen-containing functional groups, which reduces the interlayer distance and restores some van der Waals interactions. The surface of rGO is characterized by a "silk-like" or "vermiculite" morphology with significant wrinkling, folding, and overlapping. These wrinkles are more pronounced than in GO due to the rapid removal of oxygen functionalities and the resulting mechanical instability of the thin layers. The red circle indicates restacking due to restored hydrophobicity.

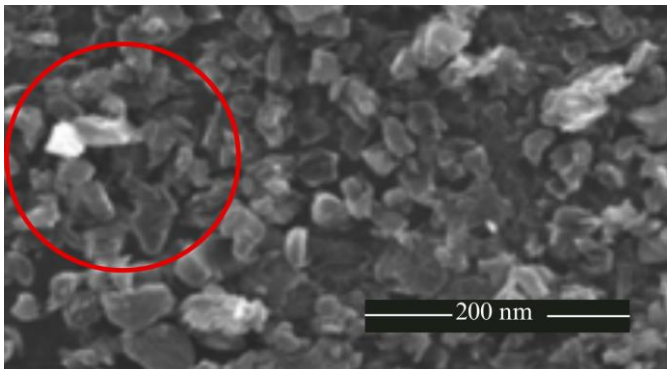

Figure 3: SEM Image of Nitrogen Doped Graphene Oxide Sample

The material maintains a clear lamellar or layered structure, indicating that the chemical exfoliation of the precursor graphite was successful and preserved during nitrogen doping in figure 3. N-GO displays a highly "silk-like" or "vermiculite" appearance with abundant surface wrinkles and folds. This texture is more pronounced than in pristine GO because the introduction of nitrogen atoms disrupts the ideal graphitic lattice, increasing mechanical instability and surface roughness.

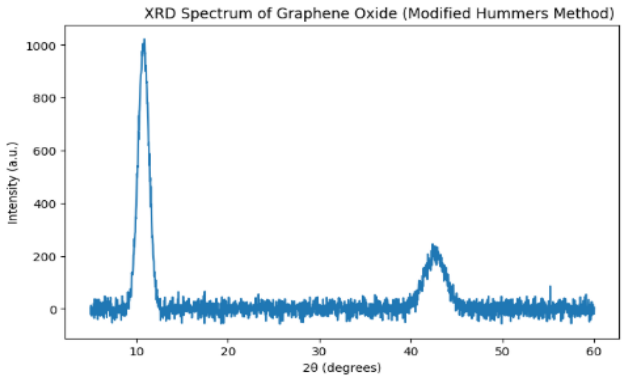

Figure 4: XRD patterns of Graphene Oxide Sample

The XRD pattern of graphene oxide (figure 4) synthesized by the modified Hummers method shows a strong (001) peak at approximately 10.8°, confirming successful oxidation and a significant increase in interlayer spacing due to the introduction of oxygen-containing functional groups. A weak feature observed around 42.6° is attributed to residual

graphitic domains, indicating that a small fraction of the sp^2 carbon framework remains intact. These results verify effective graphite oxidation while retaining limited graphitic order, which is beneficial for subsequent reduction and functionalization processes.

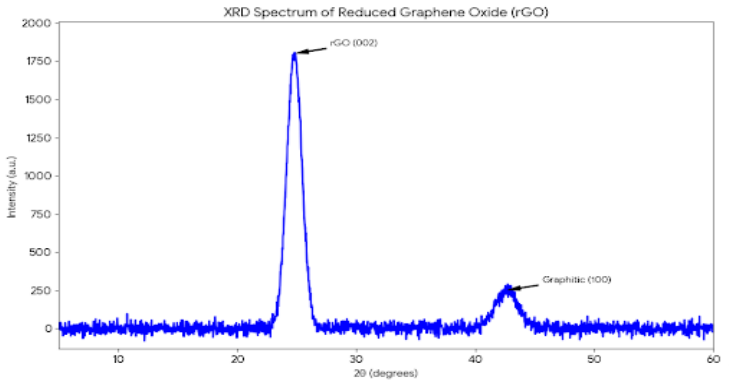

Figure 5: XRD Patterns of Reduced Graphene Oxide Sample

In figure 5, the XRD pattern of rGO displays a broad and intense peak at $2\theta \approx 24.8°$, corresponding to the (002) graphitic planes, which indicates a significant decrease in interlayer spacing compared to graphene oxide and confirms successful reduction. A weaker peak at $2\theta \approx 42.6°$, assigned to the (100) plane, suggests partial restoration of the hexagonal carbon lattice within the graphene sheets.

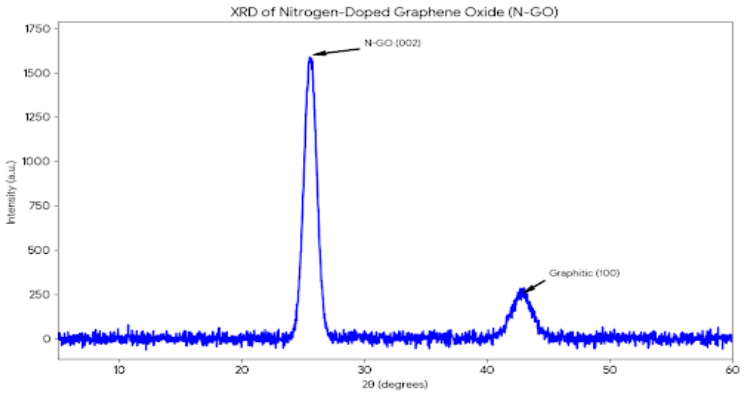

Figure 6: XRD Patterns of Nitrogen doped Graphene Oxide Sample

The XRD pattern of N-GO in figure 6 shows a prominent peak at $2\theta \approx 25.6°$, indicating effective removal of most oxygen functional groups and a significant reduction in interlayer spacing as the sheets restack into a more graphitic structure. The calculated d spacing of approximately 0.35 nm is slightly larger than that of pristine graphite, reflecting the influence of nitrogen incorporation and residual structural defects. A broad peak at $2\theta \approx 42.8°$, corresponding to the (100) plane, confirms the preservation of the hexagonal graphene lattice within the individual sheets.

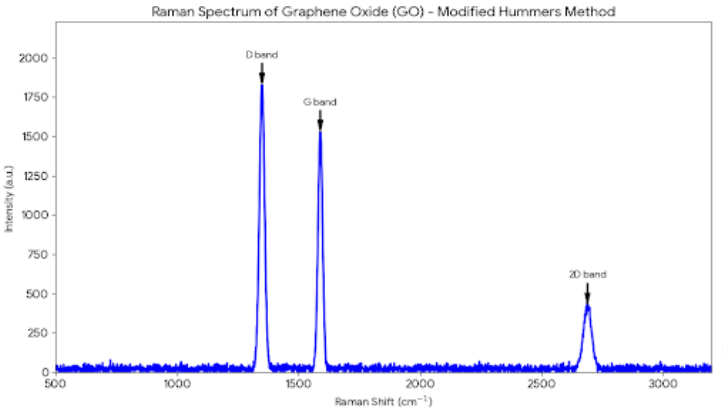

Figure 7: Raman Spectra of Graphene Oxide Sample

The Raman spectrum of GO (figure 7) indicates a strong D band at approximately 1350 cm^{-1}, indicating a high density of structural defects introduced during oxidation, mainly from oxygen-containing functional groups that disrupt the sp^2 carbon lattice. The G band near 1590 cm^{-1} corresponds to in-plane vibrations of sp^2 carbon atoms and appears broadened due to lattice distortion and strain. An ID/IG ratio of about 1.2 confirms extensive oxidation and loss of long-range graphitic order. The 2D band around 2690 cm^{-1} is weak and broad, reflecting strong disorder and localized electronic states characteristic of graphene oxide.

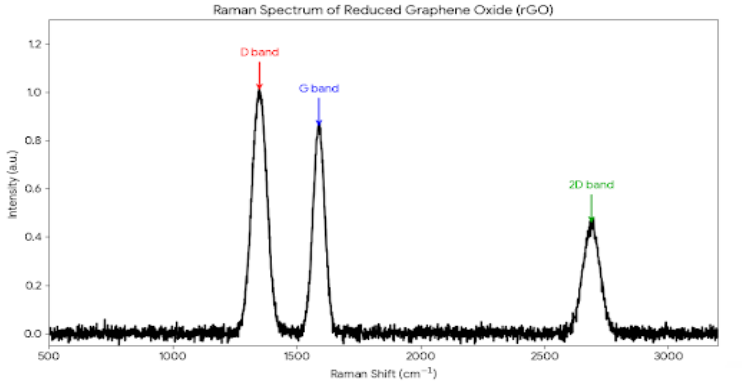

Figure 8: Raman Spectra of Reduced Graphene Oxide Sample

In figure 8, the Raman spectrum of rGO exhibits a prominent D band at 1350 cm^{-1}, indicating the persistence of structural defects and reduced sp^2 domain sizes formed during the reduction process. The G band at 1590 cm^{-1} confirms the partial restoration of the graphitic sp^2 network. An ID/IG ratio of approximately 1.18 reflects a high density of defects and edge sites, which is typical for chemically reduced graphene oxide. The 2D band at 2690 cm^{-1} appears with moderate intensity, and its clear presence compared to GO indicates improved graphitization and recovery of the sp^2 carbon lattice.

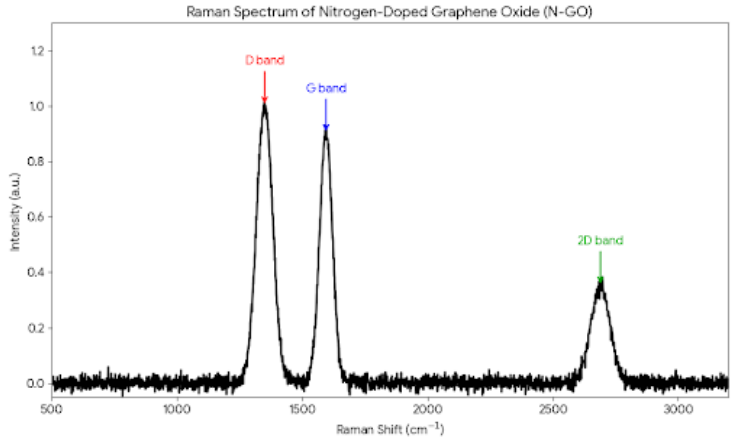

Figure 9: Raman Spectra of Nitrogen doped Graphene Oxide Sample

The Raman spectrum of N-doped GO in figure 9 shows a highly intense D band at 1350 cm^{-1}, indicating a high density of structural defects introduced by nitrogen incorporation, including pyridinic, pyrrolic, and graphitic N sites within the sp^2 framework. The G band at 1595 cm^{-1} exhibits a slight blue shift relative to GO and rGO, which is characteristic of N-doping and reflects changes in local strain and electron density. A high ID/IG ratio of approximately 1.11 confirms effective modification of the carbon lattice and increased edge and sp^3-hybridized sites. The 2D band at 2690 cm^{-1} is broad and weak, consistent with doping-induced charge carrier scattering that suppresses the resonant Raman process.

CONCLUSION

Graphene oxide (GO), reduced graphene oxide (rGO), and nitrogen-doped graphene oxide (N-GO) were systematically characterized to understand their structural and morphological evolution for electrochemical water treatment. SEM revealed that GO consists of large, thin, and highly wrinkled flakes, indicative of successful exfoliation and high surface area. rGO sheets displayed denser stacking with pronounced folding, reflecting partial restoration of graphitic order after oxygen removal. N-GO exhibited the most crumpled and defect-rich morphology, resulting from nitrogen incorporation, which enhanced surface roughness and exposed additional active sites.

XRD analysis confirmed these transformations. GO showed a strong (001) peak at ~10.8°, consistent with expanded interlayer spacing from oxygen functional groups. rGO and N-GO exhibited (002) reflections near 24–25°, reflecting reduced interlayer spacing and partial graphitic restoration, while the presence of the (100) plane in rGO and N-GO confirmed retention of the hexagonal carbon lattice.

Raman spectra complemented these findings. GO displayed a high ID/IG ratio and a weak 2D band, indicating significant disorder. rGO retained defects but showed partial graphitization with a discernible 2D band. N-GO exhibited a blue-shifted G band and a high ID/IG ratio, confirming

successful nitrogen doping and the introduction of additional defect sites.

Overall, the combined structural and morphological analyses demonstrate that N-GO possesses the most favorable features enhanced defect density, high surface roughness, and preserved graphitic domains making it the most promising candidate among the three materials for electrochemical water treatment applications.

REFERENCES

Dreyer, D. R., Park, S., Bielawski, C. W., & Ruoff, R. S. (2010). The chemistry of graphene oxide. Chemical Society Reviews, 39(1), 228–240.

Dybowski, K., Romaniak, G., Kula, P. et al. Composite carbon electrode with a coating of nanostructured, reduced graphene oxide for water electrodialysis. J Appl Electrochem 55, 131–145 (2025). DOI: https://doi.org/10.1007/s10800-024-02157-1

Ferrari, A. C., & Robertson, J. (2000). Interpretation of Raman spectra of disordered and amorphous carbon. Physical Review B, 61(20), 14095–14107.

Geng, D., et al. (2011). Nitrogen doping increases active sites for oxygen reduction reaction in carbon materials. Journal of Physical Chemistry C, 115(35), 17667–17670.

Li, P., et al. (2022). Nitrogen-doped graphene oxide with enhanced bio-electrocatalytic activity for wastewater treatment. Journal of Cleaner Production, 335, 130308.

Li, X., Cai, W., An, J., Kim, S., Nah, J., Yang, D., Piner, R., Velamakanni, A., Jung, I., Tutuc, E., Register, L. F., Banerjee, S. K., Ruoff, R. S. (2009). Large-Area Synthesis of High-Quality and Uniform Graphene Films on Copper Foils. Science, 324(5932), 1312-1314.

Liu, X., et al. (2018). Graphene-based materials for capacitive deionization. Journal of Materials Chemistry A, 6, 13882–13900.

Novoselov, K. S., Geim, A. K., Morozov, S. V., Jiang, D., Zhang, Y., Dubonos, S. V., Grigorieva, I. V., & Firsov, A. A. (2004). Electric field effect in atomically thin carbon films. Science, 306(5696), 666-669.

Pei, S., & Cheng, H.-M. (2012). The reduction of graphene oxide. Carbon, 50(9), 3210–3228.

Qu, L., Liu, Y., Baek, J.-B., & Dai, L. (2010). Nitrogen-doped graphene as efficient metal-free electrocatalyst for oxygen reduction. ACS Nano, 4(3), 1321–1326.

Stankovich, S., et al. (2007). Synthesis of graphene-based nanosheets via chemical reduction of exfoliated graphite oxide. Carbon, 45(7), 1558–1565.

Veleva, S. (2025). Mixing approaches in enhancing the capacitive performance of hybrid rGO composites. Materials, 18(11), 2460.

Voiry, D., et al. (2016). Conducting MoS_2 nanosheets as catalysts for hydrogen evolution reaction. Science, 353(6301), 1413–1416.

Zhou, M., et al. (2014). Vertically aligned graphene nanosheets for high-performance electrochemical water treatment. ACS Applied Materials & Interfaces, 6(16), 13967–13974.

Zhou, C., et al. (2024). Nondestructive analysis of plastic debris from micro to nano sizes: A state-of-the-art review on Raman spectroscopy-based techniques. TrAC Trends in Analytical Chemistry, 172, 117565..